94-352

объединенный
институт
ядерных
исследований
дубна

E2-94-352

S.G.Mashnik

PHYSICS OF THE CEM92M CODE

Invited talk presented to the NEA Nuclear Science Committee Meeting on Intermediate Energy Nuclear Data, Nuclear Energy Agency Headquarters, Issy-les-Moulineaux, Paris, May 30 — June 1, 1994

1994

1. Introduction

A large amount of nuclear reaction data at medium energies is required for different important applications, e.g., for recent plans of transmutation of long-lived radioactive wastes with a spallation source, medical and biomedical needs, and research of cosmic-ray effects on spaceships and astronauts. Experiments to measure these data are costly and there are a limited number of facilities available to make these measurements. Therefore reliable models are required to provide the necessary data.

On the other hand, for solving different purely academic problems, such as investigations of quark and gluon degrees of freedom of nuclei, one needs to estimate the role of common "background" nuclear effects, again using reliable models. One model like that may be our Cascade-Exciton Model (CEM) of nuclear reactions[1], realized in the code CEM92M. The aim of my talk is to demonstrate this, to show the main assumptions of the CEM, to summarize the parameters of the code CEM92M, and to discuss some further development and improvement of the CEM92M.

2. Basic Assumptions of the CEM and Parameters of the CEM92M

A detailed description of the CEM may be found in Ref. [1], therefore, only its basic assumptions will be outlined here. The CEM assumes that the reactions occur in three stages. The first stage is the intranuclear cascade in which primary particles can be rescattered several times prior to absorption by, or escape from the nucleus. The excited residual nucleus remaining after the emission of the cascade particles determines the particle-hole configuration that is the starting point for the second, pre-equilibrium stage of the reaction. The subsequent relaxation of the nuclear excitation is treated in terms of the exciton model of pre-equilibrium decay which includes the description of the equilibrium evaporative third stage of the reaction.

In a general case, the three components may contribute to any experimentally measured quantity. In particular, for the inclusive particle spectrum to be discussed later, we have

$$\sigma(\mathbf{p})d\mathbf{p} = \sigma_{in}[N^{cas}(\mathbf{p}) + N^{prq}(\mathbf{p}) + N^{eq}(\mathbf{p})]d\mathbf{p}. \tag{1}$$

The inelastic cross section σ_{in} is not taken from the experimental data or independent optical model calculations, but it is calculated within the cascade model itself. Hence the CEM predicts the absolute values for calculated characteristics and does not require any additional data or special normalization of its results.

An important point of the CEM is the condition for transition from the intranuclear cascade stage to the pre-equilibrium processes. In the conventional cascade-evaporation models fast particles are traced down to some minimal energy, the cutoff energy T_{cut} being about 7-10 MeV below which particles are considered to be absorbed by the nucleus. The CEM uses another criterion according to which a primary particle is considered as part of the cascade, namely the proximity of the imaginary part of the optical potential $W_{opt\,mod}(r)$ calculated in the cascade model to the experimental one $W_{opt\,exp}(r)$. This value is characterized by the parameter

$$\mathcal{P} = |(W_{opt\,mod} - W_{opt\,exp})/W_{opt\,exp}|. \tag{2}$$

In the CEM92M, we use the fixed value $\mathcal{P} = 0.3$ extracted from the analysis [1]-[4] of experimental proton- and pion-nucleus data at low and intermediate energies.

One should note that in the CEM the initial configuration for the pre-equilibrium decay (number of excited particles and holes, i.e., excitons $n_0 = p_0 + h_0$, excitation energy E_0^* and linear momentum $\mathbf{P}_0$ of the nucleus) differs significantly from that usually postulated in exciton models. Our calculations [1]-[4] show that the distributions of residual nuclei remaining after the cascade stage of the reaction, i.e., before the pre-equilibrium emission, with respect to n_0, p_0, h_0, E_0^* and $\mathbf{P}_0$ are rather broad.

Complex particles can be produced in nucleon-nucleus reactions at different interaction stages and due to many mechanisms. These may include fast processes like direct knock-out, pick-up reactions or final state interactions resulting in coalescence of nucleons into a complex particle. The CEM92M neglects all these processes at the cascade interaction stage. Therefore, fast complex particles can appear in our model only due to pre-equilibrium processes. We assume that in the course of the reaction p_j excited particles are able to condense with probability γ_j forming a complex particle which can be emitted during the pre-equilibrium state. The "condensation" probability γ_j is estimated as the integral of overlapping the wave function of independent nucleons with that of the complex particle (cluster). Of course, slow complex particles may be evaporated along with nucleons at the compound stage of the reaction. We include the emission of n, p, d, t, ^{3}He and ^{4}He at both the pre-equilibrium and the evaporative stages of reaction.

The cascade stage of the interaction is described by the Dubna version of the intranuclear cascade model (ICM) [6]. All the cascade calculations are carried out in a three-dimensional geometry. The nuclear matter density $\rho(r)$ is described by the Fermi distribution with two parameters taken from the analysis of electron-nucleus scattering. Practically, the nucleus target is divided by concentric spheres into seven zones in which the nuclear density is cônsidered to be constant. The energy spectrum of nuclear nucleons is estimated in the perfect Fermi gas approximation with the local Fermi energy $T_F(r) = \hbar^2[3\pi^2\rho(r)]^{2/3}/(2m)$, where m is the nucleon mass. The influence of intranuclear nucleons on the incoming projectile is taken into account by adding to its laboratory kinetic energy an effective real potential V, as well as by taking into account of the Pauli principle which forbids a number of intranucear collisions and effectively increases the mean path free of fast particles inside the target. For incident nucleons $V \equiv V_N(r) = T_F(r) + \epsilon$, where $T_F(r)$ is the corresponding Fermi energy and ϵ is the mean binding energy of the nucleons ($\epsilon \simeq 7$ MeV [6]). For pions, in the Dubna ICM usually one uses [6] a square-well potential with the depth $V_\pi \simeq 25$ MeV, independently of the nucleus and pion energy. The interaction of the incident particle with the nucleus comes to a series of successive quasifree collisions of the fast cascade particles (π or N) with intranuclear nucleons:

$$NN \to NN, \qquad NN \to \pi NN, \qquad NN \to \pi_1, \cdots, \pi_i NN$$
$$\pi N \to \pi N, \qquad \pi N \to \pi_1, \cdots, \pi_i N \qquad (i \geq 2) \; . \tag{3}$$

To describe these elementary collisions, one uses the experimental cross sections for the free πN and NN interactions approximated by special polynomial expressions with energy-dependent coefficients [6] and one takes into account the Pauli principle.

The Pauli exclusion principle at the cascade stage of the reaction is handled in the following way: one assumes that nucleons of the target occupy all the energy levels up to the Fermi energy. Each simulated elastic or inelastic interaction of the projectile (or of a cascade particle) with a nucleon of the target is considered forbidden if the "secondary" nucleons have energies smaller than the Fermi energy. If so, the trajectory of the particle is traced further from the forbidden point and a new interaction point, a new partner and a new interaction mode are simulated for the traced particle, and so on, until the Pauli principle is kept or the particle leaves the nucleus.

The Dubna ICM is described in detail in the monograph [6]. Let me mention briefly here some more questions related to pion absorption. Besides the elementary processes (3), the Dubna ICM takes into account also pion absorption on the nuclear pairs

$$\pi NN \to NN. \tag{4}$$

The momenta of two nucleons participating in the absorption are chosen randomly from the Fermi distribution, and the pion energy is distributed equally between these nucleons in the center-of-mass system of the pion and nucleons participating in the absorption. The direction of motion of the resultant nucleons in this system is taken as isotropically distributed in space. The effective cross section for absorption (let me speak below, for concreteness, e.g., about minus pions π^-)[1] is estimated from the experimental cross-section of pion absorption by deuterons

$$\sigma(\pi^- + \text{"}np\text{"} \to nn) = W\,\sigma(\pi^- + d \to nn) \tag{5}$$

W may be a complex function on pion energy T_π, nucleus-target, the point where the pion is absorbed, and on the spin-isospin states of absorbing pairs. Concrete calculations showed [6] that one obtains an overall satisfactory description of the data for a large range of pion energies and nuclei-targets using an "effective" approximation $W \simeq$ const $= 4$. The CEM92M uses the approximation $W = 4$, as usually in the Dubna ICM [6].

The CEM predicts forward peaked in the laboratory system angular distributions for secondary particles. Firstly, this is due to high asymmetry of the cascade component (for ejected nucleons and pions). A possibility for forward peaked distributions of nucleons and composite particles emitted during the pre-equilibrium interaction stage is related to retention of some memory of the projectile's direction. In addition to energy conservation we need to take into account conservation of linear momentum $\mathbf{P}$ at each step as a nuclear state evolves. In a phenomenological approach this can be realized in different ways [1]. The simplest way used in the CEM92M consists in sharing the momentum $\mathbf{P}_0$ (similarly to energy E_0^*) between an ever increasing number of excitons involved in the interaction in the course of equilibration of the nuclear system. In other words, the momentum $\mathbf{P}_0$ should be attributed only to n excitons rather than to all A nucleons. Then, particle emission will be symmetric in the proper n-exciton system but some forward peaking will arise in both the laboratory and center-of-mass reference frame.

The CEM was proposed initially to describe nucleon-induced reactions at bombarding energies below or at ~ 100 MeV and developed after that for a larger interval of incident nucleon and pion bombarding energies (see, e.g., [3, 4] and references given therein), for the description of stopped negative pion absorption by nuclei (see Ref. [2] and references given therein), and for the description of photonuclear reactions [5].

Recently the CEM was developed by including the competition between particle emission and fission at the evaporative stages of reactions [7]. Six different versions of the liquid-drop

[1] The corresponding formulae for π^+ absorption may be easily obtained by simple replacements $\pi^- \to \pi^+$, $n \to p$, $p \to n$, $N \to Z$ and $Z \to N$

model (LDM), single-Yukawa modified LDM, and Yukawa-plus-exponential modified LDM, and two phenomenological approaches are incorporated in the CEM92M. Two different excitation energy dependences of fission barriers and two dependences of fission barriers on angular momenta of fissioning nuclei are incorporated in the CEM92M. Three different models for shell and pairing corrections are incorporated in the CEM92M (for details see Ref. [7]).

Recently the CEM was also developed [8] by including a more realistic nuclear level density (with Z, N, and E^* dependences of level density parameter). Eight parametrizations for level density parameters $a(Z, N, E^*)$ are incorporated in the CEM92M (for details see Ref. [8]). Every incorporated model for fission barriers, shell and pairing corrections, level density parameter a may be easily selected by input switches.

At present we develop the CEM for the description of the possibility of γ-emission at all three stages of a reaction [9]. The corresponding recent modified version of the code is named CEM94.

In the CEM92M all the CEM parameter values are fixed and are the same as in Ref. [1].

3. Exemplary Results and Discussion

We analyzed and evaluated a large variety of data from nucleon-, pion-, and $\gamma-$induced reactions using the CEM (see Refs.[1]-[5], [7]-[10] and references given therein). A detailed comparison of the CEM92M predictions with the results of other current models may be found in the recent review [11]. Therefore, I confine myself to the discussion of some exemplary results. Measured [12] and calculated inclusive spectra of protons are shown in Fig. 1. The CEM92M reproduces well the change in the spectrum shape with increasing emission angle and in passing from light to heavy target-nuclei, providing correct absolute values for the particle yield for all incident energies.

To illustrate the relative role of different proton production mechanisms for neutron-copper collisions at 425 MeV, as an example, the cascade, pre-equilibrium and the evaporative components of proton spectra are shown separately in the upper part of Fig. 2. One can see that the main contribution of slow protons to the spectra comes from the evaporation from compound nuclei, while with increasing ejectile energy the emission at the cascade and pre-equilibrium stages becomes dominant. The cascade component describes almost the entire measured spectra at forward angles but with increasing angle of detection the relative role of the pre-equilibrium component rises considerably, and for very backward angles and proton energies less than 80 MeV the contribution of pre-equilibrium emission becomes comparable with that from the cascade. For lighter nuclei the pre-equilibrium processes are less important but for heavier targets the pre-equilibrium emission contributes more essentially to the hard part of backward emitted particle spectra than for Cu ones. The observed spectra of protons correspond to the sum of all three CEM components; therefore there is an agreement for energy spectra in both the shape and absolute value over the entire range of angles and energies of ejectiles.

For many applications and scientific problems it is necessary to analyze and evaluate not only data on nucleon production, but also other characteristics, as data on complex particle and pion production, fission cross section. Some exemplary results are shown in Figs. 3 - 5.

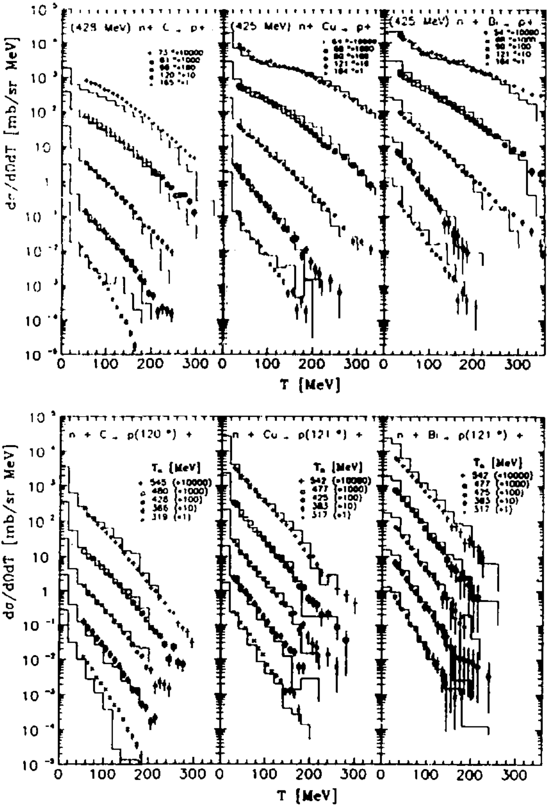

Fig. 1. Measured [12] inclusive proton spectra (symbols) and CEM92M calculations (histograms). Different emission angles (upper row) and different incident energies (lower row) are drawn with symbols as indicated. The histograms are the sum of all three CEM (cascade, preequilibrium and evaporative) components.

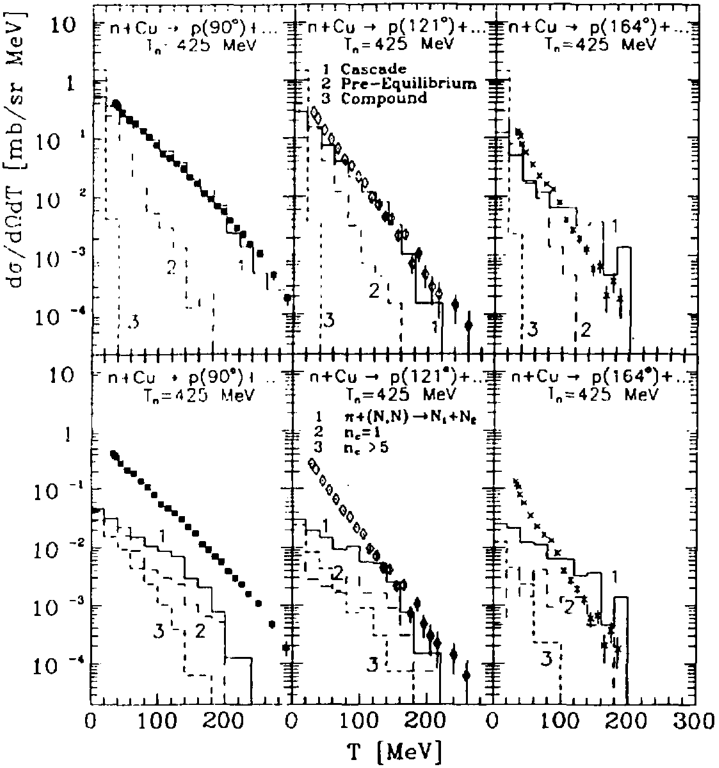

Fig. 2. Inclusive proton spectra from the neutron-copper collisions at 425 MeV. **Upper row:** the histograms 1, 2, and 3 show the contribution of cascade, pre-equilibrium, and evaporative components, respectively; **lower row:** for cascade component the histograms 1, 2, and 3 show the contribution from events which contain a two-step process of pion production in collisions of incident or cascade particles with nuclear nucleons (3) followed by pion absorption on nucleon pairs within this target-nucleus (4) in the course of the reaction (including all possible former and/or subsequent intranuclear collisions), the contribution from the events with $n_c = 1$, and $n_c > 5$, respectively. The value n_c is the number of successive interaction acts before proton emission in the events contributing to the corresponding histograms. The experimental points are taken from Ref. [12].

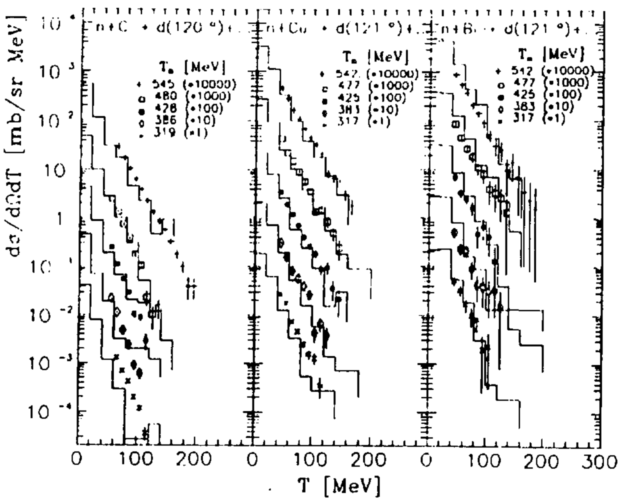

Fig. 3. Inclusive deuteron spectra; histograms are the sum of pre-equilibrium and evaporative components calculated within the CEM, the rest notation is the same as in Fig. 1.

Fig. 3 shows inclusive spectra of deuterons measured [12] and calculated with the CEM92M with fixed value for the level density parameter: $a = 0.1A$ and without taking into account paring effects and fission processes. The low energy parts of the complex particle spectra calculated in the CEM are formed by particles evaporated at the compound stage of the reaction, while the high energy ones are determined by the pre-equilibrium emission. It can be seen that the CEM reproduces correctly the shape and the absolute value of the backward complex particle spectra. To describe better the complex particle spectra at these intermediate energies we should take into account the dependence of the level density parameter a on the excitation energy E^* of nuclei and calculate more carefully the "condensation" probabilities γ_j.

The CEM predicts a major contribution to the measured complex particle spectra from the pre-equilibrium processes and for fast backward emitted particles this contribution is comparable with the experimental data. For forward angles the CEM significantly underestimates the experimental data (see, e.g., Ref. [4]). This happens because we neglect in our approach fast processes of complex particle production such as pick-up, knock-out and coalescence of complex particles from fast nucleons emitted during the cascade stage. Such processes contribute especially to the forward complex particle emission and their disregard in the CEM92M results in such an underestimation of complex particle spectra at forward angles. To describe better the complex particle spectra at intermediate energies the CEM92M must be improved by incorporating fast processes of complex particle production. It is planed to make such a development of the CEM92M in the future.

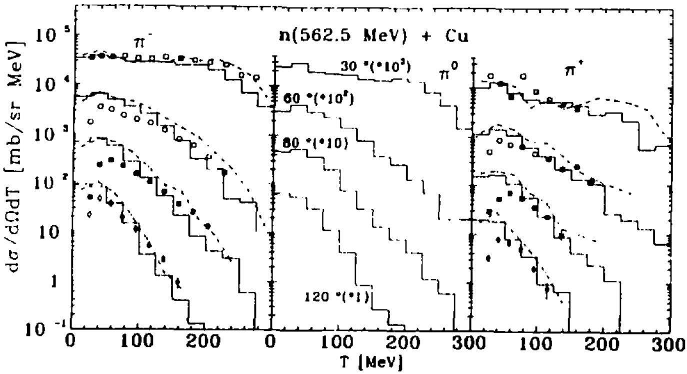

Fig. 4. Double differential cross sections at angles 30°, 60°, 80°, and 120° of three pion charge states for 562.5 MeV neutrons on Cu. The points are experimental data [13], the histograms and dashed lines are our CEM92M and LAHET [14] calculations from Ref. [13], respectively.

I have applied the CEM92M to analyze practically all known data on nucleon-induced pion production for intermediate and heavy nuclei and bombarding energies less than several GeV. As an example, Fig. 4 shows a part of the recent data [13] on neutron-induced inclusive π^- and π^+ production along with our CEM92M and LAHET [14] calculations from ref. [13]. For comparison, spectra of neutral pions predicted by the CEM92M are also shown in the figure. One can see that both the CEM and Bertini's ICM give results in reasonable agreement with the data. Similar agreement was obtained for other reactions.

Recently I have applied the CEM92M to analyze nucleon-, pion-, and photon-induced fission. As an example, the incident energy dependences of experimental and calculated with the CEM92M fission cross-sections for proton-gold and -uranium interactions are shown in Fig. 5. I performed these calculations with Cameron's [15] shell and pairing corrections, third Iljinov, Mebel's et al. [16] systematics for the level density parameter, Krappe, Nix and Sierk's [17] fission barriers with the dependences $B_f(E^*)$ proposed by Barashenkov et al. [18], by Sauer et al. [19], as well as without a dependence of B_f on E^*. The values used for the ratio a_f/a_n are shown in the figure. One can see that by choosing the corresponding values for the ratio a_f/a_n the CEM reproduces correctly the shape and the absolute value of the fission cross-sections in the interval of bombarding energies regarded here, independently of the form of the dependence $B_f(E^*)$ used in the calculations. Analogous results have been obtained also for other targets.

Our analysis has shown that very voluminous but uncoordinated experimental data on fission processes obtained by now in separate measurements do not permit one to discriminate various models for fission barriers and to determine simultaneously the value of the ratio a_f/a_n. New complex data on fission processes, measured simultaneously with the characteristics of all emitted particles and fragments for such reactions where the fission cross-section is of the

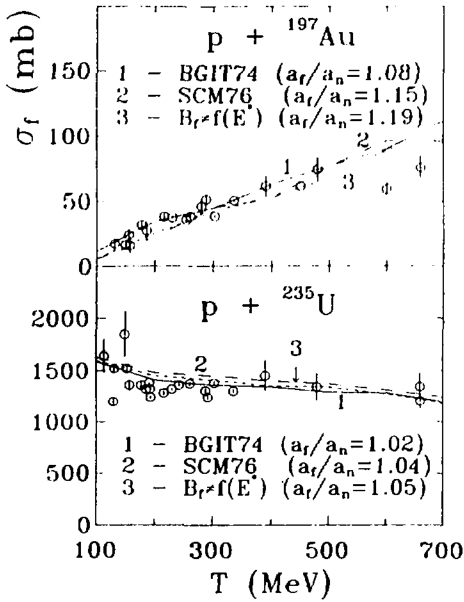

Fig. 5. Incident energy dependence of fission cross-sections for proton-gold and proton-uranium interactions. The experimental points are from the summary Table 159 of the monograph [6]. The lines are our CEM92M calculations performed with different fission barriers (for details see Ref. [7]) for the values of a_f/a_n shown in the figure.

same order of magnitude with the particle- and fragment-production cross-sections, and the analysis of all these data in a unique approach may clear up these questions. Such "complete" measurements are possible and desirable in the near future at the FOBOS setup at the Flerov Laboratory of Nuclear Reactions of the Joint Institute for Nuclear Research (Dubna). A paper with a detailed analysis of fission processes in the framework of the CEM is in preparation.

For many applications and scientific problems pion-induced reactions are as important as those of nucleons. I have analyzed, in our CEM, different characteristics of pion-nucleus interactions in the incident pion energy range from 0 MeV to 3 GeV (see, e.g., [2, 3, 10]). For our model there is no difference between nucleon- and pion-induced reactions. The first step of the cascade stage of the reaction is simply induced by a pion instead of a nucleon. As an example, a part of Golubeva's et al. data [20] are presented in Fig. 6 along with my CEM92M calculations and results of the best fit [20] in the moving-source model. For comparison, for

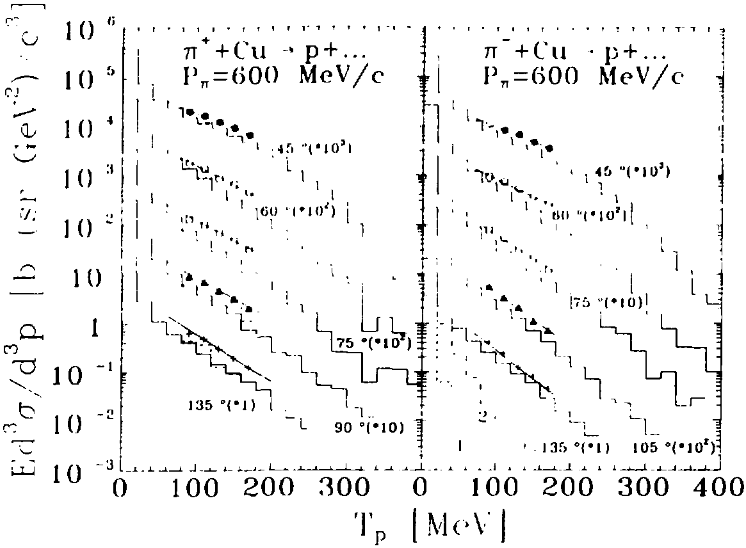

Fig. 6. Measured inclusive proton spectra from π^+ and π^- interactions with copper at 600 MeV/c [20] (symbols), our CEM92M calculations (solid histograms are sums of all three CEM components), the results of the best fit in the moving-source model [20] (lines), and the calculations with the Dubna ICM with Δ as cascade participants from Ref. [20] (dashed histograms on the left graph). The dashed histograms 1 and 2 on the right graph show the CEM evaporative and preequilibrium components for the angle 135°, respectively.

proton spectra from 600 MeV/c π^+ interactions with Cu the results of the Dubna ICM calculation with the Δ isobar production in the intermediate states from ref. [20] are shown in Fig. 6. One can see that both our CEM and the ICM equally satisfactorily describe the data.

For spectra at 135°, the CEM preequilibrium and evaporative components are shown separately in Fig. 6. One can see that even at these relatively high incident energies the preequilibrium processes contribute to intermediate energy proton emission. But for $T_p > 80$ MeV the emission of cascade protons becomes dominant, and the preequilibrium components lie one order of magnitude lower than the data.

To describe better the pion-nucleus interactions in the Δ resonance region, the CEM92M must be improved by including the dependence of V_c on pion momentum and on radius, a more proper description of the cross sections of elementary processes (5) of the genuine pion absorption by nucleon pairs, and by including in our classical approach quantum corrections and medium effect (for details see Ref. [21]). Such a work is in progress at present.

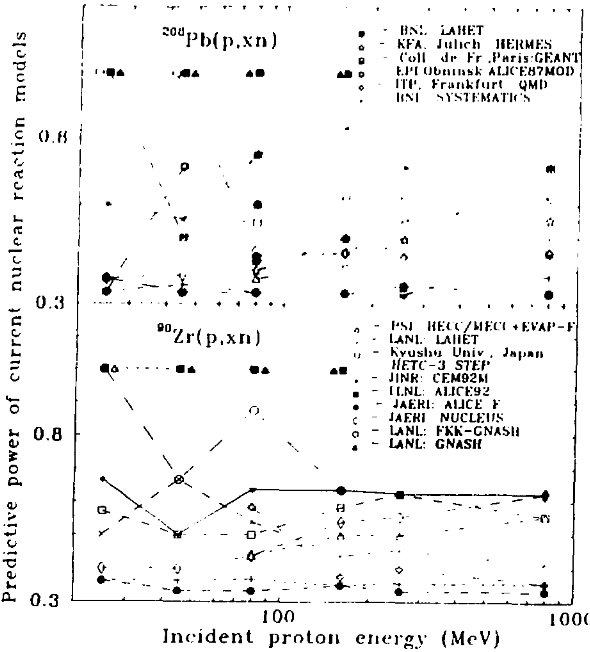

Fig. 7. Predictive power of different codes involved in the recent "International Code and Model Intercomparison for Intermediate Energy Reactions" [11] (for details see text).

As it was mentioned above, a most complete comparison of the CEM92M predictions with calculations in the framework of other current models may be found in the recent review on *International Code Comparison for Intermediate Energy Nuclear Data* [11]. *This review* contains the detailed results of calculations carried out by eighteen laboratory groups involved in nuclear reaction modeling. The calculations cover incident proton energies from 25 MeV to 1600 MeV on targets of Zirconium and Lead. Because of the very large amount of information, the authors of the review [11] have tried to provide an overview (in Table 5 and 6) giving a figure of merit for each calculation at each incident energy and angle. This "figure of merit" grade of 1, 2, or 3 was given (by two knowledgeable physicists who were not participants in this exercise) subjectively with the following guideline:

Grade (1)	If the calculation followed the data quite well over the full energy range, almost always within a factor of two discrepancy or less.
Grade (2)	The calculation is generally within a factor of two of the data, occasionally outside this regime, and the shape roughly follows experimental results.
Grade (3)	The calculated results were outside the above limits.

Results of the two "beauty contest" judges were summed to produce Tables 5 and 6 of review [11].

It is clear that the predictive powers of the codes involved in this exercise are as the inverse of the "figures of merit" shown in Tables 5 and 6 of review [11], lie in the range from 1/3 to 1, although this is a gross oversimplification. Using these "figures of merit", I averaged over the angles regarded in calculations the number of marks of each value per code for each incident energy of this intercomparison exercise. Then I calculated the "predictive power" of each code as the inverse of this averaged "figure of merit". Fig. 7 shows these predictive powers as functions of incident proton energy. On can see that the CEM92M has the best predictive power as compared to other codes involved in this intercomparison at incident energies higher than 160 MeV. At lower incident energies the calculated predictive power of the CEM92M is a little bit worse, although remains still as one of the best. This can be explained by the fact that to economize the computing time I performed the calculations for this intercomparison using fixed values for the level density parameter: $a = 0.1A$, $a = 0.125A$, and $a = 0.05A$, for Zr, W, and Pb targets, respectively, without taking into account shell and pairing effects, and fission processes. At high incident (and excitation) energies the effects of nuclear structure are inessential and the approach used in my calculations provided the best predictive power for the CEM92M. To have similar predictive power at lower energy one needs to perform calculations using a more realistic nuclear level density (with Z, N, and E^* dependences of level density parameter) and taking into account shell and pairing corrections. The CEM92M allows one to perform easily such calculations by selecting input switches but requires more computing time.

4. Summary

Without any free parameters the CEM92M is able to reproduce correctly shapes and absolute values of a large variety of nucleon- and pion-induced reactions data. The recent "International Code and Model Intercomparison for Intermediate Energy Reactions" [11] showed that the CEM92M adequately describes nuclear reactions at intermediate energies and has one of the best predictive powers as compared to other available modern codes.

A recent modified version of the code of our model named CEM93 allows one to calculate also photonuclear reactions data.

A more recent modified version of the code named CEM94 is able to describe also emission of gamma rays and has an input simple and friendly for users. It is planned to make these versions available to users. A detailed description (User Manual) of the recent modified versions of the code is in preparation.

One may conclude that the Cascade-Exciton Model is indeed suitable for the evaluation of medium energy nuclear data for science and applications. Further development and improvement of the CEM codes are possible, and such a work is in progress at present.

References

[1] K.K. Gudima, S.G. Mashnik and V.D. Toneev, Nucl. Phys. A401 (1983) 329; JINR Communications P2-80-774, P2-80-777, Dubna (1980)

[2] S. G. Mashnik, Revue Roum. Phys. 37 (1992) 179;
Proc. 20th Winter School Leningrad Inst. Nucl. Phys., vol. 3 (Leningrad, 1985) p. 236;
Preprint ICTP, Miramare-Trieste IC/92/39 (1992)

[3] V.I. Komarov et al., Nucl. Phys. **A326** (1979) 297;
S.G. Mashnik and S Tesch, Z. Phys. **A312** (1983) 259,
S.G. Mashnik, in: Proc. 18th Winter School Leningrad Inst. Nucl. Phys., vol. 3 (Leningrad, 1983) p. 172;
S.G. Mashnik, S. Tesch and S.V. Dzemuhadze, Preprint Inst. Appl. Phys. 84-3, Kishinev (1984);
V.N. Baturin et al., Preprint LINP-1302, Leningrad (1987);
K.K. Gudima, S.G. Mashnik and V.D. Toneev, JINR Communication E2-11307, Dubna (1978)

[4] S.G. Mashnik, Nucl. Phys. **A568** (1994) 703

[5] F.G. Gereghi, V.A. Zolotarevsky, K.K. Gudima, S.G. Mashnik and L.V. Bordianu, Calculation of Cross Sections for Photoneutron Reactions (Kishinev, Kishinev State University, 1990) in Russian

[6] V.S. Barashenkov and V.D. Toneev, Interaction of High Energy Particles and Nuclei with Atomic Nuclei (Atomizdat, Moscow, 1972) in Russian

[7] S.G. Mashnik, Acta Phys. Slov. **43** (1993) 243

[8] S.G. Mashnik, Acta Phys. Slov. **43** (1993) 86

[9] S.G. Mashnik, Ye.S. Golubeva and A.S. Iljinov, "Gamma Emission Calculation in the Cascade-Exciton Model", Proc. Int. Conf. on Perspectives for the Interaction Boson Model on the Occasion of Its 20th Anniversary, Padova, Italy, June 13-17, 1994

[10] S.G. Mashnik, Acta Phys. Pol. **B24** (1993) 1685

[11] M. Blann, H. Gruppelar, P. Nagel and J. Rodens, International Code Comparison for Intermediate Energy Nuclear Data (OECD, Paris, 1994)

[12] J. Franz et al., Nucl. Phys. **A510** (1990) 774

[13] M.L. Brooks et al., Phys. Rev. **C45** (1992) 2343

[14] H.W. Bertini, Phys. Rev. **188** (1986) 1711;
R.E. Prael and H. Lichtenstein, Los Alamos National Laboratory version of the HETC Monte Carlo code which was originaly developed at Oak Ridge National Laboratory, LA-UR-89-3014, (1989)

[15] A.G.W. Cameron, Can. J. Phys. **35** (1957) 1021

[16] A.S. Iljinov, M.V. Mebel et al., Nucl. Phys. **A543** (1992) 517

[17] H.J. Krappe, J.R. Nix and A.J. Sierk, Phys. Rev. **C20** (1979) 992

[18] V.S. Barashenkov, F.G. Gereghi, A.S. Iljinov and V.D. Toneev, Nucl. Phys. **A222** (1974) 204

[19] G. Sauer, H. Chandra and U. Mosel, Nucl. Phys. **A264** (1976) 221

[20] M.B. Golubeva et al., Proc. 5th All-Union Sem. Program of Experimental Infestigations at the Meson Factory of the Inst. Yad. Isled. Akad. Nauk SSSR, Zvenigorod, April 12-15, 1987, (Moscow, Inst. Yad. Isled. Akad. Nauk SSSR, 1987), p.205, in Russian

[21] S.G. Mashnik, JINR Preprint E2-93-470, Dubna (1993); submitted to Yad. Fiz.

Received by Publishing Department
on September 2, 1994.